

Alcoholysis of Furfuryl Alcohol into *n*-Butyl Levulinate Over SBA-16 Supported Heteropoly Acid Catalyst

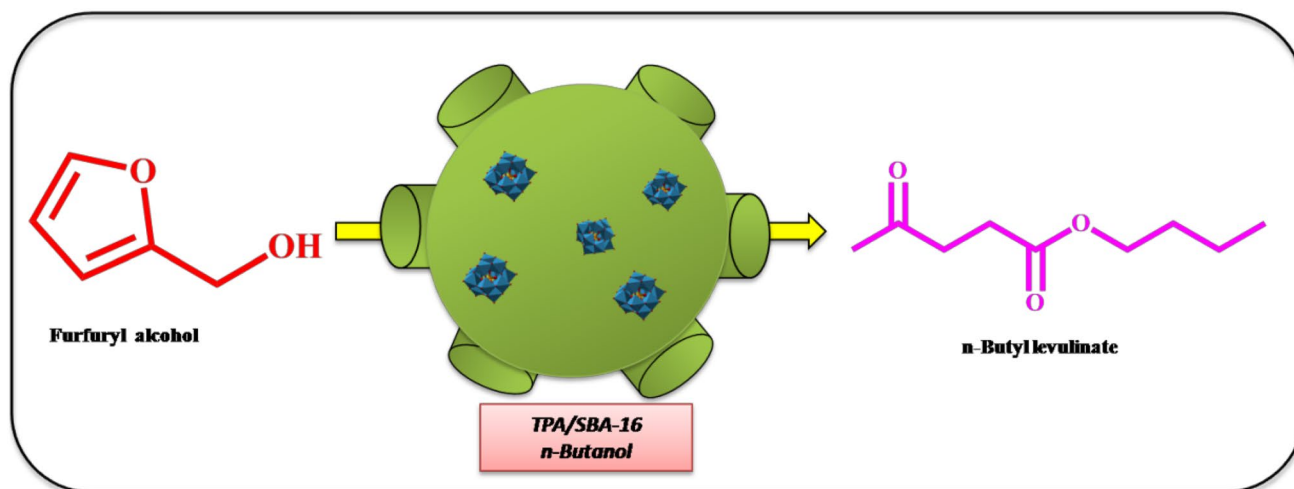
Enumula Siva Sankar¹ · K. Saidulu Reddy¹ · Yadagiri Jyothi¹ · Burri David Raju¹ · Kamaraju Seetha Rama Rao¹

Received: 4 May 2017 / Accepted: 1 August 2017
© Springer Science+Business Media, LLC 2017

Abstract In this work, *n*-butyl levulinate a potential renewable chemical in the energy sector and in the field of fine chemical synthesis has been synthesized via alcoholysis of furfuryl alcohol in batch process at atmospheric pressure over SBA-16 supported tungstophosphoric acid (TPA) catalyst. In order to characterize and correlate the catalytic activity, the wet impregnated TPA/SBA-16 catalysts were subjected to the physico chemical characterization techniques such as X-ray diffraction, N₂-physisorption, SEM, TEM, FT-IR, NH₃-TPD and pyridine adsorbed FT-IR analysis. The retention of 3D mesoporous structure and TPA

structure even after impregnation was confirmed by XRD and N₂-physisorption. The impregnation of TPA over SBA-16 creates the more number of available active acidic sites for the reactants. 25 wt% TPA/SBA-16 offers 97% selectivity to *n*-butyl levulinate with complete conversion of furfuryl alcohol in 3 h. Various reaction parameters were optimized to achieve the best catalytic activity. These results imply that the conversion of furfuryl alcohol to *n*-butyl levulinate go on with the formation of the intermediate 2-butoxymethylfuran. The recyclability of the catalyst and characterization of the spent catalyst was also studied.

Graphical Abstract



✉ Kamaraju Seetha Rama Rao
ksramarao@iict.res.in; ksramarao.iict@gov.in

¹ Inorganic and Physical Chemistry Division, CSIR-Indian Institute of Chemical Technology, Hyderabad 500007, India

SBA-16 supported TPA catalyst is effective in the conversion of furfuryl alcohol to *n*-butyl levulinate at atmospheric pressure.

Keywords Furfuryl alcohol · *n*-Butanol · TPA · SBA-16 · *n*-Butyl levulinate

1 Introduction

Alkyl levulinates are biomass derived renewable chemicals possessing potential applications in the field of synthesis of fine chemicals and transportation fuel industry. The active organic functional groups i.e. keto and ester groups made alkyl levulinates as successful precursors in the plastic industry, flavoring and fragrance industries [1]. In particular, *n*-butyl levulinate (BL), oxygenate of second generation fuel or fuel additive has received much more attention due to its versatile characteristics. BL has high oxygen content, low solubility in water, high octane number and physical properties which are similar to diesel fuel [2]. Methyl tert-butyl ether (MTBE) used in the transportation fuels, which is water soluble carcinogen can be replaced by BL due to its promising fuel additive properties [3]. Owing to the fascinating properties of BL, its synthesis is gaining interest among the biomass conversions. The synthesis of alkyl levulinates can be done from raw biomass, carbohydrates, levulinic acid and furfuryl alcohol (FA) [4–7]. The conversion of FA into alkyl levulinates via alcoholysis with alcohols is advantageous in terms of cost and easy reactivity of FA in alcoholysis reaction with alcohols [8, 9]. BL synthesis was reported from alcoholysis of FA with *n*-butanol in presence of homogeneous acid catalysts [10–12]. Due to environmental and recyclability issues the homogeneous acid catalysts replacement by solid acid catalysts is beneficial. Several catalytic systems have been applied towards the synthesis of BL from FA such as double SO₃H-functionalized ionic liquids [11], sulfonic acid functionalized ionic liquids [13], organic inorganic hybrid catalyst ([MIMBS]₃PW₁₂O₄₀) [14], Al-TUD-1 [15], ion exchange resins, zeolites [16] etc. Even though, these catalytic systems offer good results, there is a need to develop an efficient solid acid catalytic system with simple catalyst preparations, cost effective and easy recovery of the catalyst after this reaction. Mesoporous silica (SBA-16) due to its large surface area, 3D cage like pore structure, thermal stability, has been attracting the catalysis community towards its application as a favorable support in various catalytic applications like adsorption, biomass conversions, drug delivery and organic transformations [17–20]. Tungstophosphoric acid (TPA) is a heteropoly acid that offers strong acidity and high oxidizing potential to catalyze acid catalyzed reactions and oxidation reactions. Though TPA's acidity helps to catalyze the reactions, its applicability is limited due to its lower surface area, thermal stability and solubility in polar solvents. These disadvantages can be avoided or minimized by dispersing the TPA on solid supports like silica, alumina, zirconia, titania, tin oxide which make the TPA as insoluble and high surface area catalytic system [21–24]. SBA-16 supported TPA catalysts would offer more number of accessible acidic sites for the conversion of FA to alkyl levulinates. In this context,

SBA-16 supported TPA catalysts were prepared by simple wet impregnation method and applied for the alcoholysis of FA with alcohols at atmospheric pressure.

2 Experimental

2.1 Catalyst Preparation

SBA-16 mesoporous silica was prepared by using F127 (EO₁₀₆PO₇₀EO₁₀₆, supplied by M/s. Sigma–Aldrich chemicals, USA) as a template, tetra ethyl ortho silicate (TEOS, M/s. Sigma–Aldrich chemicals, USA) as silica source and *n*-butanol as co-surfactant. In a typical synthesis, to a solution of 3.5 g of F127 dissolved in 175 mL of 0.4 M HCl, 13 mL of *n*-butanol was added with stirring at 45 °C. After 1 h stirring, 16.7 g of TEOS was introduced into the mixture and then stirred for 20 h followed by static hydrothermal treatment at 100 °C for 24 h. It was filtered and the solid mass was dried at 100 °C for 12 h. The white solid was calcined at 550 °C for 6 h in flow of air and the resultant solid (SBA-16) was used as support [25, 26]. SBA-16 supported catalysts were prepared by wet impregnation method. Requisite amount of TPA dissolved in water was added to the SBA-16 support and it was dried on a hot plate with stirring until complete dryness. The solid was kept in air oven at 100 °C for 12 h and then it was calcined at 300 °C for 2 h. The resultant solid was labeled as XTS where X stands for the weight percentage of TPA.

2.2 Characterization of Catalysts

The N₂ physisorption-desorption studies were performed for the samples after degassing them at 150 °C for 2 h (M/s. Quanta chrome Instruments, USA) with nitrogen as adsorbate at liquid N₂ temperature. The X-ray diffraction studies of the samples were carried out on an Ultima-IV diffractometer (M/s. Rigaku Corporation, Japan), equipped with nickel-filtered Cu K α radiation ($\lambda = 1.54056 \text{ \AA}$). The electron microscopic images were recorded on a scanning electron microscope (M/s. JEOL, Switzerland) for SEM (scanning electron microscope) images and on a JEM 2000EXII apparatus (M/s. JEOL, Switzerland) for TEM (transmission electron microscope) images. Before TEM analysis, the samples were ultra sonicated in ethanol and a drop was placed on carbon coated copper grid and then ethanol was evaporated in an air oven at 80 °C. Fourier transform IR spectra were recorded on spectrum GX spectrometer (M/s. Perkin-Elmer, Germany) within the scan range of 1400–400 cm⁻¹. The pyridine adsorption FT-IR patterns were recorded in the diffuse reflectance infra red Fourier transform (DRIFT) mode. In the characteristic experiment the sample was degassed under vacuum at 200 °C for 3 h followed by suspending

in dry pyridine. Then, the sample was heated at 120 °C for 1 h. At room temperature, FT-IR spectra of the pyridine-adsorbed samples were recorded. The temperature programmed desorption of ammonia (NH₃-TPD) was performed on homemade reactor equipped with a gas chromatograph having TCD detector. In a typical experiment, about 50 mg of catalyst sample was placed in a tubular quartz reactor. The catalyst sample was pre-treated in a flow of helium at 300 °C for 1 h. After pretreatment the catalyst sample was saturated with 10% NH₃/He at 80 °C for 30 min. Subsequently, helium was allowed to flush for 30 min at 100 °C to remove physisorbed ammonia. Helium flow was continued with increasing the temperature to 800 °C at a ramp of 10 °C min⁻¹ and the desorbed NH₃ was monitored by the TCD equipped gas chromatograph which was connected with standard GC software.

2.3 Catalytic Activity

The catalytic activity of SBA-16 supported TAP catalysts were evaluated for the alcoholysis of FA with *n*-butanol at atmospheric pressure. In a typical procedure, 1 mmol of FA and 6 mL of *n*-butanol along with 0.3 g of catalyst (catalyst to substrate ratio is 3.05) were taken in 25 mL round bottom flask equipped with a reflux condenser. The mixture was heated at temperature range of 70–130 °C for 3 h. The reaction conditions are same in all the reactions unless otherwise specified. The analysis of the reaction mixture was performed on a FID equipped GC GC-17A (M/s. Shimadzu Instruments, Japan, EB-5 capillary column, 30 m × 0.53 mm × 5.0 μm) and the products were confirmed by GC-MS, QP-2010 (M/s. Shimadzu Instruments, Japan, EB-5MS capillary column, 30 m × 0.25 mm × 0.25 μm).

3 Results and Discussion

The low angle X-ray diffraction patterns of the catalyst samples were shown in Fig. 1a. All the catalysts exhibit three diffractions at 2θ values of around 0.8°, 1.0° and 1.2° due to (110), (200) and (211) planes respectively, these diffraction peaks are the characteristic peaks for the mesoporous materials with 3D cubic (Im3m) structure [25, 26]. The $d_{(110)}$ and a_0 values were presented in Table 1 and are in accordance with the mesoporous 3D materials [25–27]. These results suggest that all the SBA-16 supported TPA catalyst samples have maintained the 3D mesoporous cubic pore arrangement of parent SBA-16. The decrease in the intensities of the diffraction peaks of the catalyst samples with increasing TPA loading can be ascribed due to the lowering of local order, due to the decrease of scattering difference between the channel walls of the matrices [29, 30]. The wide angle XRD patterns (From Fig. 1b) of the SBA-16 and SBA-16 supported TPA catalysts show a broad peak at 2θ values between 15–30° which indicates the presence of amorphous silica [26]. Along with the broad peak, there are low intense signals at 2θ values of around 10.4°, 21.2°, 26.1°, 30.2° and 34.9° in the SBA-16 supported TPA catalysts representing the presence of Keggin heteropoly acid structure and signifying that the TPA is in highly dispersed form over the SBA-16 [31, 32]. The intensity of the indexed diffraction planes increases with the loading of TPA on SBA-16. This can be attributed that at lower loadings of TPA, it is in highly dispersed (below the detection limit of XRD) or may be in amorphous form. At higher TPA loadings, the indexed diffraction planes are due to the formation of the crystallite phase of TPA.

Figure 2a shows the N₂ adsorption–desorption isotherms of the SBA-16 and SBA-16 supported TPA catalyst samples. All the catalyst samples demonstrate the type IV isotherm

Table 1 Textural and structural parameters of SBA-16 and TPA/SBA-16 samples

Catalyst	S_{BET}^a (m ² g ⁻¹)	V_t^b (cc/g)	D^c (nm)	$d_{(110)}^d$ (nm)	a_0^e (nm)	t^f (nm)	Acidity (mmol NH ₃ /g)
SBA-16	707	0.51	2.99	9.85	13.93	10.94	0.03
5TS	405	0.30	2.89	10.19	14.41	11.52	0.52
10TS	403	0.29	3.00	10.31	14.58	11.57	0.96
15TS	416	0.29	2.98	10.28	14.53	11.55	1.43
20TS	383	0.27	2.93	10.51	14.86	11.93	1.92
25TS	216	0.16	3.01	10.27	14.52	11.51	2.17
30TS	194	0.14	2.97	10.36	14.65	11.68	2.31

^aBET Surface area

^bTotal pore volume

^cAverage pore size

^dPeriodicity of SBA-16 derived from a low angle XRD

^eUnit cell parameter = 2^{1/2} $d_{(110)}$

^fPore wall thickness = (3^{1/2} $a_0/2$) – D

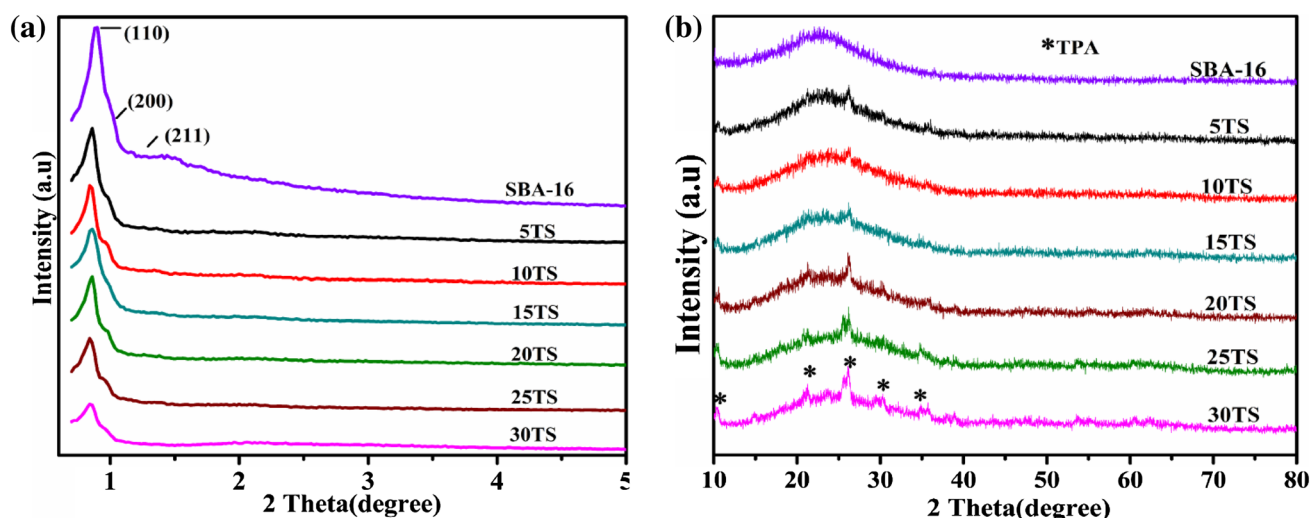


Fig. 1 a Low angle XRD patterns of pristine SBA-16 and TPA/SBA-16 samples; b wide angle XRD patterns of TPA/SBA-16 samples

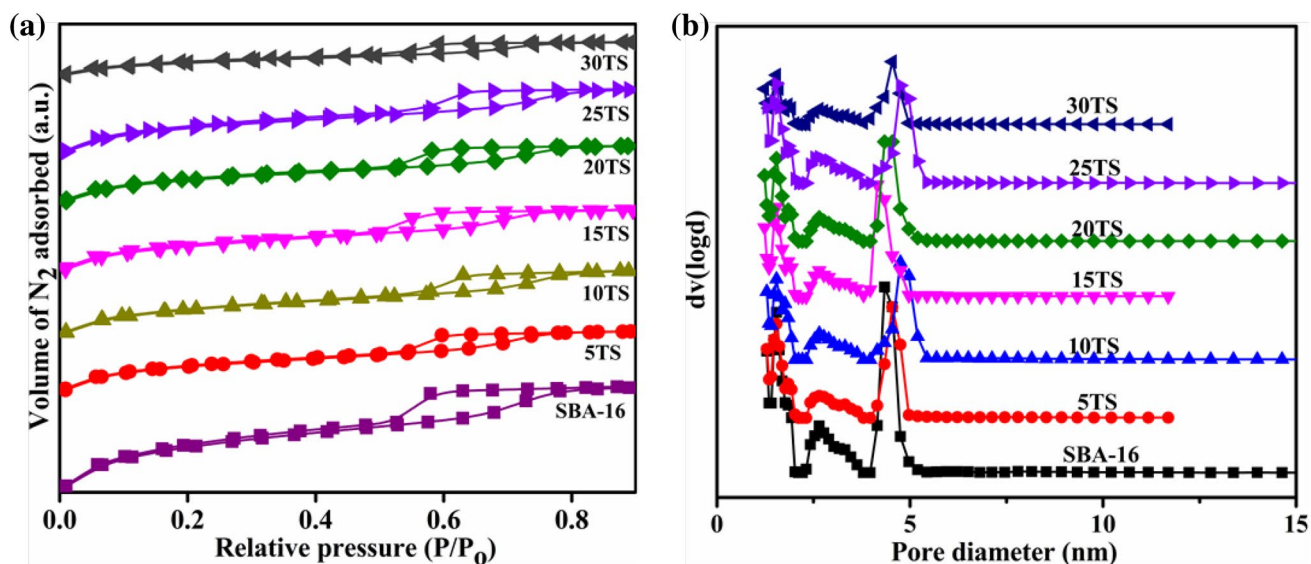


Fig. 2 a N_2 adsorption–desorption isotherms for pristine SBA-16 and TPA/SBA-16 samples; b pore size distribution of pristine SBA-16 and TPA/SBA-16 samples

with H2 hysteresis loop of IUPAC classification of porous materials indicating cage like pore structured mesoporous materials [25–27]. The capillary condensation takes places within the P/P_0 range of ~ 0.5 – 0.8 which validate the retention of mesoporous structure of SBA-16 even after TPA impregnation. The textural features of the samples are presented in Table 1. Figure 2b displays bimodal pore size distributions of these samples with an average pore size of ~ 4.5 nm indicating of cage type mesopores [25–27].

The morphological features of the SBA-16 and 25TS catalysts were investigated by electron microscopic studies and

the images were presented in Fig. 3. SEM images of SBA-16 and 25TS catalyst samples show agglomerated spheres like morphology in both the samples in accordance with the reported literature [26, 27]. TEM images of SBA-16 and 25TS catalyst samples show well organized pore channels in addition to this, the 25TS catalyst shows the presence of well dispersed form of TPA over SBA-16 [26–28].

The strength of the acidic sites present in the catalyst can be assessed by the NH_3 -TPD analysis. Depending upon the desorption temperature of NH_3 , the acidic sites are classified as weak acidic sites (<250 °C), moderate acidic sites

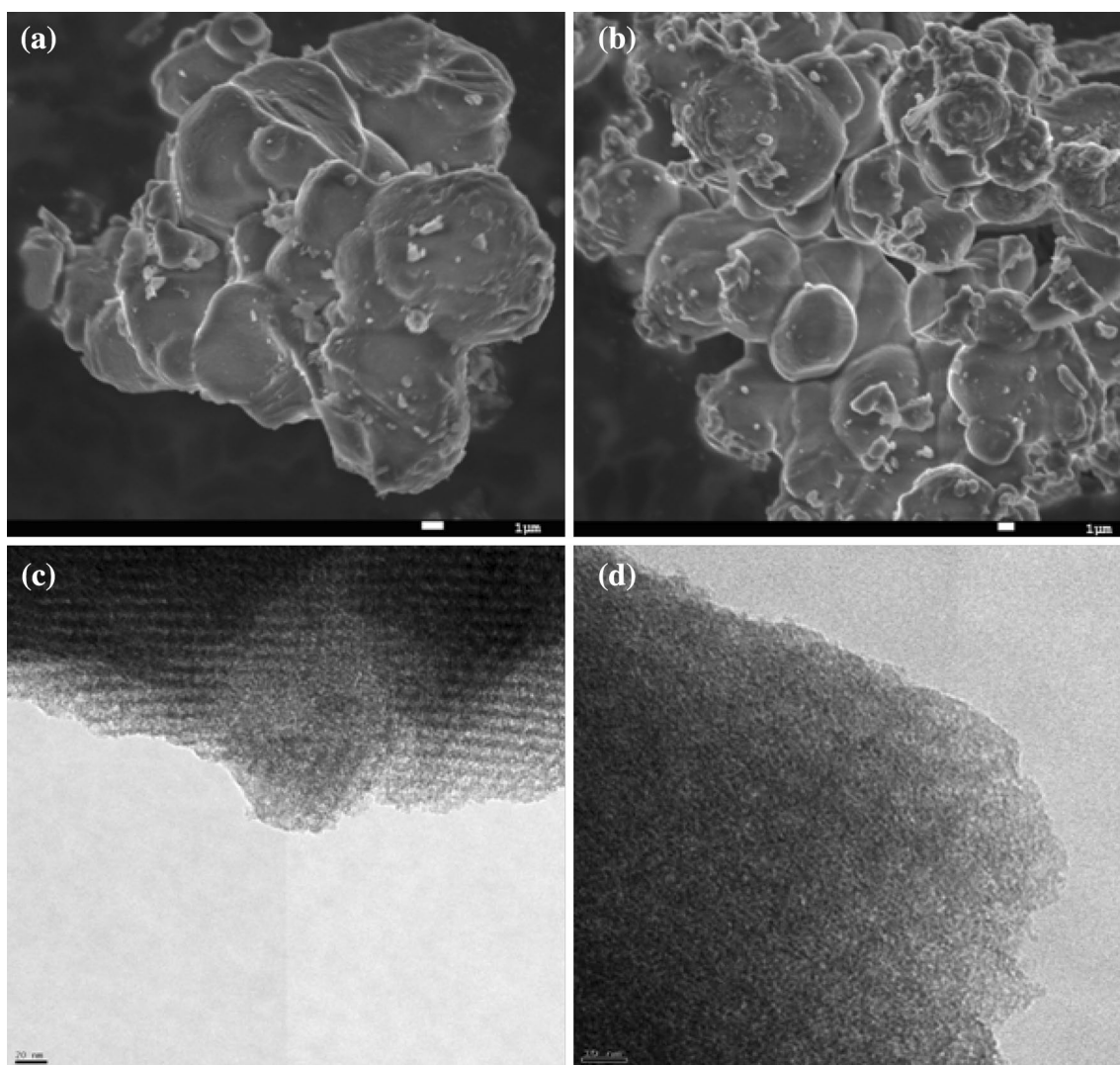


Fig. 3 SEM images of (a) pristine SBA-16 (b) 25TS TEM images of (c) pristine SBA-16 and (d) 25TS

(250–400 °C) and strong acidic sites (>400 °C) [33–35]. Figure 4 displays the NH_3 -TPD profiles of the catalysts. SBA-16 supported TPA catalysts show two desorption peaks in the temperature region of 150–250 °C and 430–600 °C representing presence of the weak and strong acidic sites respectively. The desorption peaks intensity is increasing with the TPA loading. The impregnation of TPA over SBA-16 enhances the number of available acidic sites (both weak and strong) and the enhancement is linear with the amount of TPA loading.

The pyridine adsorbed FT-IR studies were conducted for SBA-16 and SBA-16 supported TPA catalyst samples to assess the type of acidic sites present in the catalysts and the patterns were illustrated in Fig. 5a. The characteristic bands at 1443 and 1589 cm^{-1} are due to the presence of surface Lewis acidic sites and the bands at 1538, 1635 cm^{-1}

are due to the protonated pyridine bonded to surface Brønsted acid sites present in the catalyst samples [36, 37]. The band at 1485 cm^{-1} in the pyridine FT-IR patterns is due to the presence of both Lewis and Brønsted acid sites in the catalyst [38]. The dispersion of TPA over SBA-16 increases both the surface Lewis and Brønsted acid sites over SBA-16 thereby increases the probability of accessibility of the acidic sites to the reactants. In order to know the stability of the acidic sites, the NH_3 -desorption spectra of the active catalyst (25TS) with different temperature was recorded and presented in Fig. 5b. The intensities of corresponding bands representing the Lewis and Brønsted acidity are decreasing after out gassing at increasing temperatures from 50 to 200 °C. But there exist bands due to the presence of surface Lewis and Brønsted acidic sites even at 200 °C.

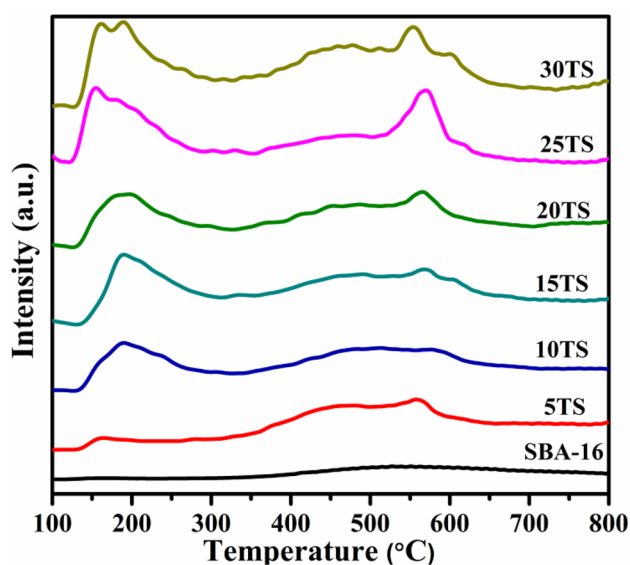


Fig. 4 NH_3 -TPD profiles of SBA-16 and TPA/SBA-16 samples

3.1 Catalytic Activity

3.1.1 Effect of TPA Loading

Figure 6 shows the effect of TPA loading on the alcoholysis of FA with *n*-butanol. The alcoholysis of FA with *n*-butanol over bare SBA-16 and TPA result in lowering the selectivity to BL (nil and 64% respectively) due to their insufficient acidity and lack of acidic site density. Whenever the alcoholysis of FA with *n*-butanol was performed over SBA-16

supported TPA catalysts, the selectivity to BL raises with increasing TPA loading. The dispersion of TPA over SBA-16 made the resultant catalysts with well accessible acidic sites for the reactants. The selectivity to BL increases from 12 to 97% as the TPA loading increases from 5 to 25 wt% and afterwards there is no significant change in the selectivity to BL. The selectivity to the intermediate, 2-butoxymethylfuran (BMF) (Scheme 1) is declining as the TPA loading is increasing, indicating that at lower loadings the presence of insufficient number of acidic sites are unable to convert the intermediate into the BL. Further, it can be observed that the desorption of NH_3 in the high temperature region (430–600 °C, From the NH_3 -TPD) increases with the loading of TPA and it is more pronounced in the case of 25TS and 30TS. It is reflected in the catalytic activity, the selectivity to BL is increased sharply from 20TS to 25TS. These results indicate the strength of the acidic sites also has influence on the alcoholysis of FA to BL.

3.1.2 Effect of Reaction Temperature

The influence of reaction temperature on the alcoholysis of FA with *n*-butanol was studied over 25TS catalyst within the temperature range 70–130 °C and the results were presented in the Fig. 7 As the reaction temperature increases from 70 to 110 °C the selectivity to BL increases from 35 to 97% and further increase in the reaction temperature to 130 °C don't show any significant increase in the selectivity to BL. Whereas the selectivity to the intermediate BMF is decreasing with the raise in reaction temperature. These results suggest that the conversion FA is consistent with the

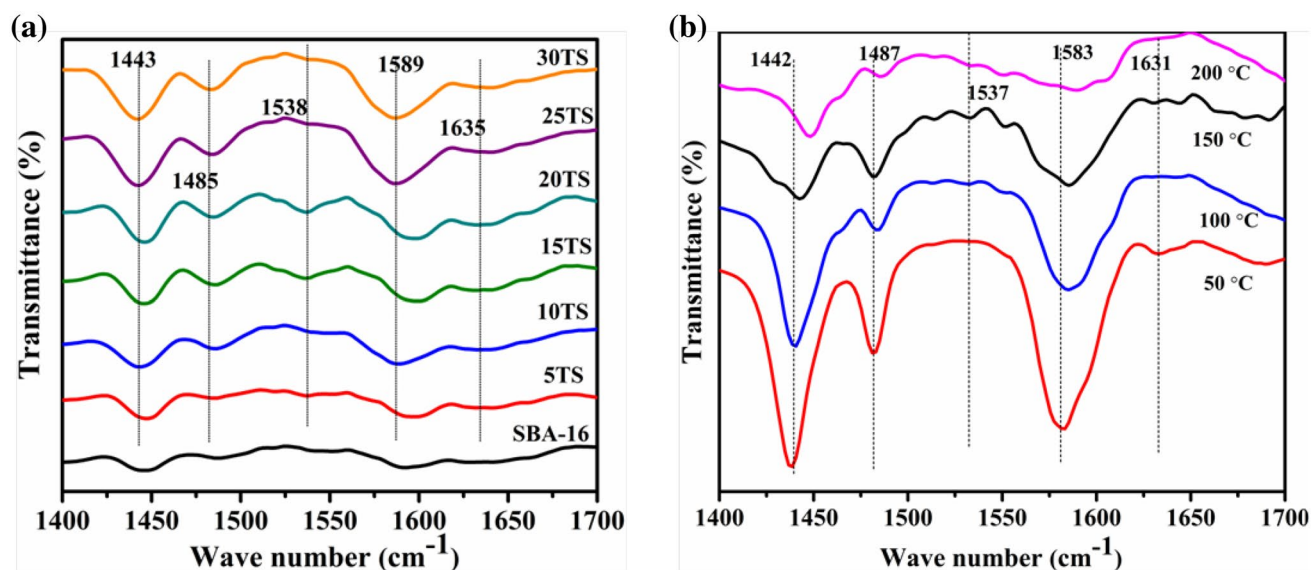


Fig. 5 **a** Pyridine adsorbed FT-IR spectra of SBA-16 and TPA/SBA-16 samples; **b** pyridine desorption spectra of 25TS catalyst at different temperatures

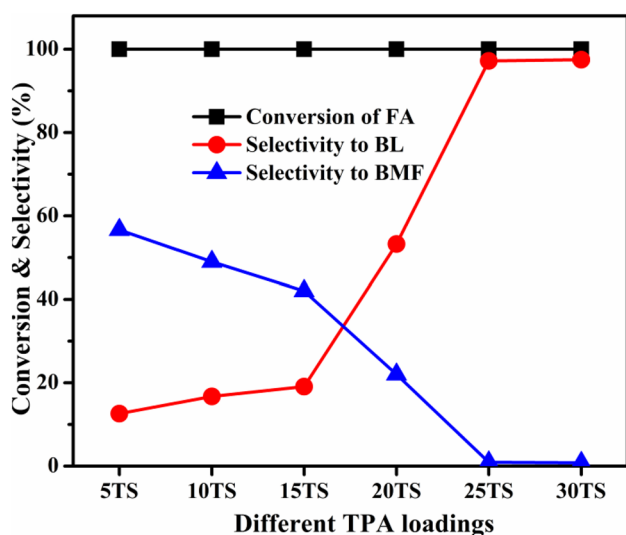


Fig. 6 Effect of TPA loading on the alcoholysis of FA. Reaction conditions: catalyst amount: 0.3 g, FA: 1 mmol, *n*-butanol: 6 mL, temperature: 110 °C, time: 3 h

reaction temperature but the conversion of the intermediate is dependent on the reaction temperature. When the reaction temperature raises from 90 to 110 °C the drastic decrease in the selectivity to the intermediate, BMF can be observed indicating the reaction temperature plays crucial role on the conversion of intermediates to BL. The optimum reaction temperature to attain the maximum selectivity to BL in this reaction is 110 °C.

3.1.3 Effect of Catalyst Amount

Figure 8 shows the influence of the catalyst amount on the conversion of FA to BL over 25TS catalyst. It can be observed that as the catalyst amount increases from 0.1 to 0.3 g, the selectivity to BL increases from 27 to 97% and further increase in the catalyst amount to 0.4 g, the selectivity to BL remains the same. With the increase in the catalyst amount from 0.1 to 0.3 g the selectivity to BMF decreases from 48 to 2%, The decrease in the selectivity to BMF with increasing catalyst amount implies that the increase in catalyst amount increases the number of available acidic sites to the reactants thereby increases the conversion of intermediates to the product, BL.

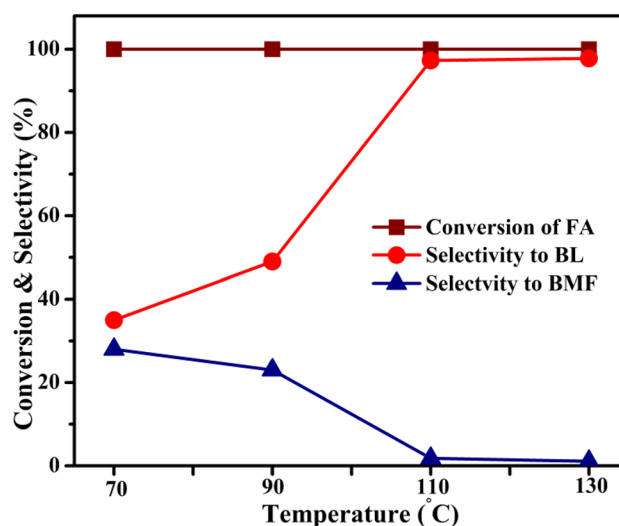


Fig. 7 Effect of temperature on the alcoholysis of FA. Reaction conditions: catalyst amount: 0.3 g, FA: 1 mmol, *n*-butanol: 6 mL, time: 3 h

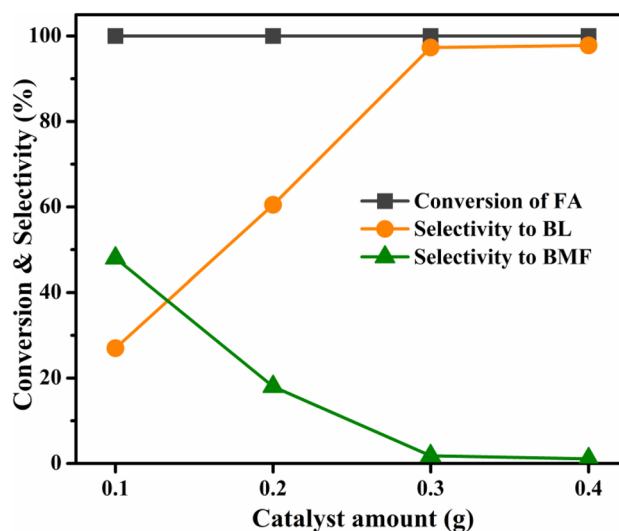
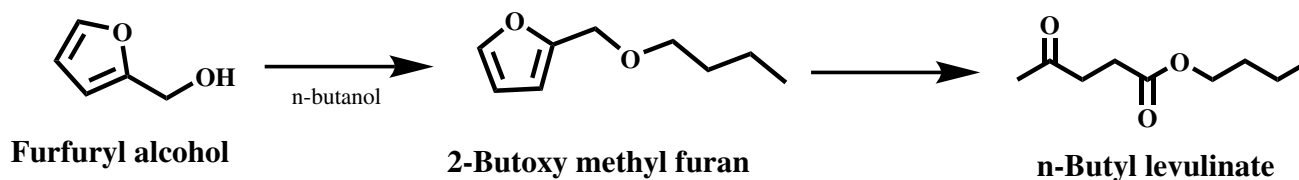


Fig. 8 Effect of catalyst amount on the alcoholysis of FA. Reaction conditions: FA: 1 mmol, *n*-butanol: 6 mL, temperature: 110 °C, time: 3 h



Scheme 1 Conversion of furfuryl alcohol into *n*-butyl levulinate

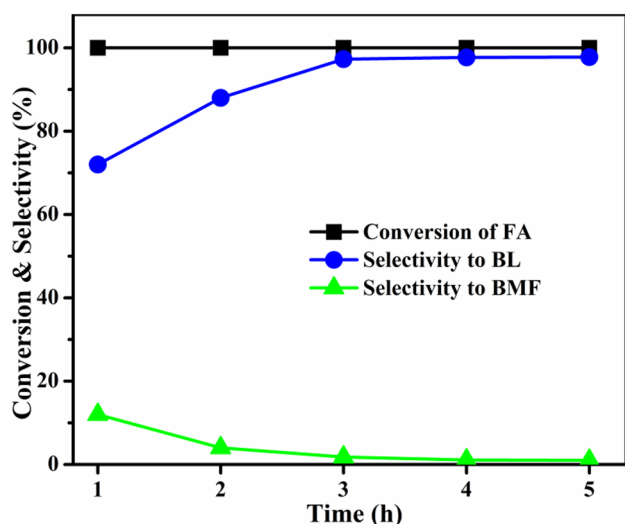


Fig. 9 Effect of reaction time on the alcoholysis of FA. Reaction conditions: catalyst amount: 0.3 g, FA: 1 mmol, *n*-butanol: 6 mL, temperature: 110 °C

3.1.4 Effect of Reaction Time

The effect of reaction time on the conversion of FA to BL over 25TS catalyst was studied over different time intervals up to 5 h and the results were illustrated in Fig. 9. After 1 h the selectivity to BL reaches to 72% with complete conversion of FA. As the reaction progresses the selectivity to BL increases to a maximum of 97% after 3 h and with further increase in the reaction time there is no considerable change in the selectivity to BL. Even though complete conversion of FA occurs within 1 h, maximum selectivity to BL is obtained after 3 h. The selectivity to the intermediate, BMF is decreasing as the reaction time increases. These results demonstrate that the conversion of FA to BL involves fast conversion of FA into the intermediate and then conversion of intermediate to the final product, BL is the rate determining step.

3.1.5 Effect of *n*-Butanol Amount

The effect of *n*-butanol amount on the conversion of FA into BL was examined over 25TS catalyst by varying the *n*-butanol volume from 2 to 8 mL and the results were presented in Fig. 10. When the reaction was performed with 2 mL of *n*-butanol the selectivity to BL is 59% and selectivity to the intermediates is 24% with complete conversion of FA. When the *n*-butanol volume increases to 4 mL the selectivity to BL increases to 80% and reaches a maximum of 97% with 6 mL of *n*-butanol and then level off. The increase in selectivity to BL with increase in the *n*-butanol volume indicates that at higher concentration of FA, it undergoes self reactions forming oligomeric products instead of

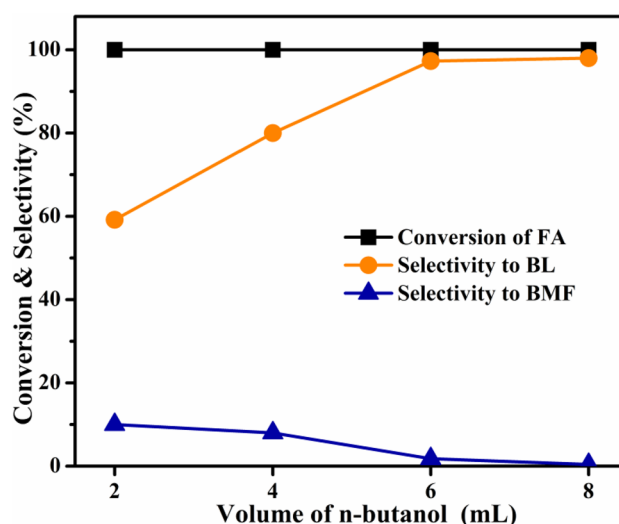


Fig. 10 Effect of *n*-butanol volume on the alcoholysis of FA. Reaction conditions: catalyst amount: 0.3 g, FA: 1 mmol, temperature: 110 °C, time: 3 h

reaction with the *n*-butanol. Hence a dilute concentration of FA is necessary to perform the alcoholysis reaction with *n*-butanol.

3.1.6 Influence of Different Alcohols

The effect of different alcohols on the alcoholysis of FA was evaluated at their reflux temperatures over 25TS catalyst and the results were presented in Fig. 11. The alcoholysis of FA with methanol, ethanol, *n*-propanol and *n*-butanol yields corresponding alkyl levulinates with selectivity's 8, 20, 77 and 97% respectively with complete conversion of FA in each case. The low selectivity to alkyl levulinates with methanol (70 °C) and ethanol (80 °C) is due to that the lower reaction temperatures which are not sufficient to form the intermediate and to convert the intermediates, alkoxy methyl furan into the product alkyl levulinate. Lower reaction temperature is the reason for the lower selectivity of alkyl levulinate in this alcoholysis of FA.

3.1.7 Recyclability of the Catalyst

The catalytic efficiency of 25TS catalyst was evaluated by conducting catalyst cycles under optimized reaction conditions and the results were shown in Fig. 12. The catalyst recovered after each catalytic cycle from the reaction mixture by centrifugation was washed with methanol and dried at 100 °C for 3 h then was used for the next catalytic run. The complete conversion of FA was observed up to four cycles while the selectivity to BL was decreased from 97 to 84%. The spent catalyst was characterized by XRD, NH₃-TPD and CHNS analysis to find out reason for the decline in the

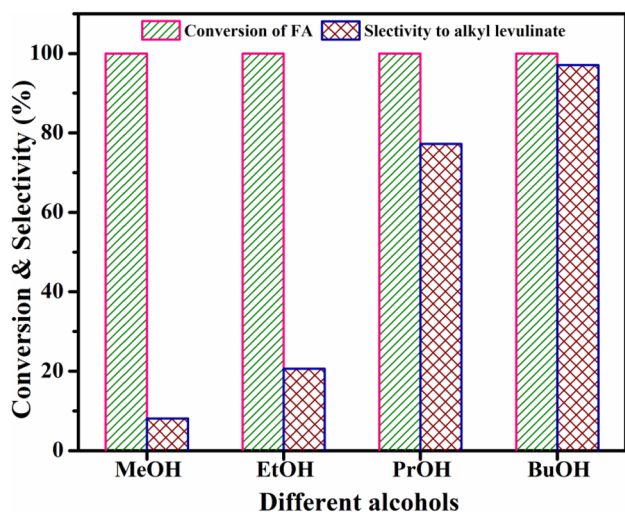


Fig. 11 Effect of different alcohols on the alcoholysis of FA. Reaction conditions: catalyst amount: 0.3 g, FA: 1 mmol, alcohol: 6 mL, time: 3 h temperature: methanol (70 °C), ethanol (80 °C), propanol (100 °C) butanol (110 °C)

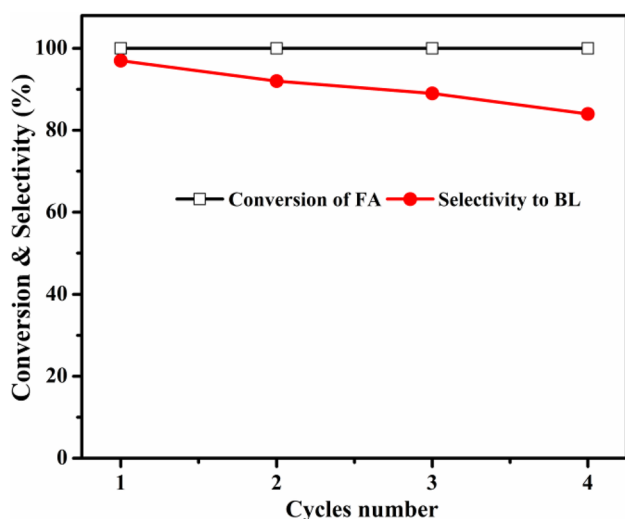


Fig. 12 Reusability of the catalyst. Reaction conditions: catalyst amount: 0.3 g, FA: 1 mmol, *n*-butanol: 6 mL, temperature: 110 °C, time: 3 h

catalytic activity. From the XRD patterns, (Fig. 13) it can be noticed that the mesoporous structure as well as TPA structure of 25TS catalyst is preserved and no structural changes were observed. NH_3 -TPD analysis shows decrease in the acidity from fresh catalyst (2.17 mmol NH_3/g) to spent catalyst (1.8 mmol NH_3/g). CHNS analysis shows the presence of carbon and hydrogen in the spent catalyst. These results suggest that the decrease in the selectivity to BL is due to the accumulation of carbonaceous species over the catalyst surface and which decreases the accessibility of the

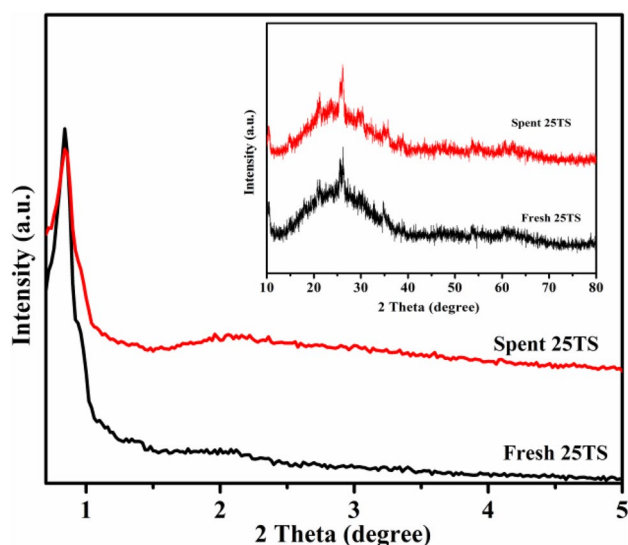


Fig. 13 XRD patterns of fresh and spent 25TS catalysts

active sites for the reactants. The heterogeneous nature of this catalytic reaction was confirmed by conducting the filtration test during the reaction. Under optimized reaction conditions, the reaction was performed for 1 h and then the catalyst was removed from the system and then continued the reaction without the addition of catalyst for another 2 h. The results after the reaction without catalyst show no accountable change in the selectivity to BL (<2%). It clearly demonstrates the heterogeneous nature of the catalyst in this reaction.

4 Conclusions

In conclusion, SBA-16 supported TPA catalysts were prepared successfully by wet impregnation method and their catalytic activity was evaluated for the conversion of FA into *n*-butyl levulinate in batch process. The characterization techniques such as XRD, N_2 -physisorption, SEM, TEM and FT-IR confirmed the retention of 3D mesoporous structure and TPA structure in the resultant catalysts. The acidic nature of these catalysts was studied by NH_3 -TPD and pyridine adsorbed FT-IR, demonstrate presence of weak and strong acidic sites and development of surface Lewis and Brønsted acidic sites over SBA-16 after dispersing TPA. These physico-chemical features play a vital role in the selective formation of BL. 25TS catalyst is found to be optimum in achieving 97% selectivity to BL with complete conversion of FA. The formation of BL occurs via the intermediate, BMF. The catalyst can be recycled up to 4 cycles and decrease in the selectivity to BL is due to the blockage of active sites by carbonaceous species.

Acknowledgements The authors SSE, SRK, JY thank UGC, New Delhi, for financial assistance.

References

- Alexandre D, Nadine E, Franck R (2014) *ACS Sustain Chem Eng* 2:1338
- Kashinath ASA, Abdul MZ, Hashim H, Wan Alwi SR (2012) *Comput Chem Eng* 41:88
- Fagan PJ, Korovessi E, Manzer LE, Mehta R, Thomas SM (2003) (DuPont) International Patent No. WO 03/085071 A1
- Siva Sankar E, Kumara Swamy K, Ramesh Babu GV, Raju BD, Rama Rao KS (2017) *Sustain Energy Fuels* 1:644
- Srinivasa Rao B, Krishna Kumari P, Dhanalakshmi D, Lingaiah N (2017) *J Mol Catal A* 427:80
- Lincui P, Lu L, Junhua Z, Jianbin S, Shijie L (2011) *Appl Catal A* 397:259
- Siva Sankar E, Mohan V, Suresh M, Saidulu G, David Raju B, Rama Rao KS (2016) *Catal Commun* 75:1
- Hayes DJ (2009) *Catal Today* 145:138
- Yao-Bing H, Tao Y, Meng-Chao Z, Hui P, Yao F (2016) *Green Chem* 18:1516
- Lock RH, Reynolds K (1955) Patent GB735693
- Lincui P, Hui L, Long X, Keli C, Haiyan C (2014) *BioResources* 9(3):3825
- Wang G, Zhang Z, Song L (2014) *Green Chem* 16:1436
- Hengne AM, Kamble SB, Rode CV (2013) *Green Chem* 15:2540
- Zhang Z, Dong K, Zhao Z (2011) *ChemSusChem* 4:112
- Patrícia N, Margarida MA, Patrícia AR, Joana PA, Sérgio L, Auguste F, Martyn P, Sílvia MR, Maria FR, Anabela AV (2013) *Green Chem* 15:3367
- Lange JP, Van de Graaf WD, Haan RJ (2009) *ChemSusChem* 2:437
- Kruk M, Jaroniec M, Sayari A (1997) *Langmuir* 13:6267
- Mohan V, Venkateshwarlu V, Saidulu G, David Raju B, Rama Rao KS (2015) *RSC Adv* 5:57201
- Zhang L, Zhu W, Lin Q, Han J, Jiang L, Zhang Y (2015) *Int J Nano Med* 10:3291
- Hao Y, Chong Y, Li S, Yang H (2012) *J Phys Chem C* 116:6512
- Raveendra G, Rajasekhar A, Srinivas M, Sai Prasad PS, Lingaiah N (2016) *Appl Catal A* 520:105
- Abd El, Rahman SK (2008) *Appl Catal A* 343:109
- Jagadeeswaraiiah K, Balaraju M, Sai Prasad PS, Lingaiah N (2010) *Appl Catal A* 386:166
- Srinivas M, Raveendra G, Parameswaram G, Sai Prasad PS, Lingaiah N (2016) *J Mol Catal A* 413:7
- Kleitz F, Kim TW, Ryoo R (2005) *Langmuir* 22:440
- Siva Sankar E, Ramesh Babu GV, Raji Reddy Ch, David Raju B, Rama Rao KS (2017) *J Mol Catal A* 426:30
- Stevens WJJ, Lebeau K, Mertens M, Tendeloo GV, Cool P, Vansant EF (2006) *J Phys Chem B* 110:9183
- Andrade GF, Soares DCF, Almeida RK, Sousa EMB (2012) *J Nanomater* 2012:816496
- Anand N, Reddy KHP, Swapna V, Rama Rao KS, David Raju B (2011) *Microporous Mesoporous Mater* 143:132
- Limand MH, Stein A (1999) *Chem Mater* 11:3285
- Dias JA, Caliman E, Dias SCL, Paulo M, De Souza ATCP (2003) *Catal Today* 85:39
- Ramesh Kumar Ch, Venkateswara Rao KT, Sai Prasad PS, Lingaiah N (2011) *J Mol Catal A* 337:17
- Mohan V, Venkateshwarlu V, Pramod CV, Raju BD, Rama Rao KS (2014) *Catal Sci Technol* 4:1253
- Boreave A, Auroux A, Guimon C (1997) *Microporous Mater* 11:275
- Ramesh Kumar Ch, Jagadeeswaraiiah K, Sai Prasad PS, Lingaiah N (2012) *ChemCatChem* 4:1360
- Bhuiyan TI, Arudra P, Akhtar MN, Aitani AM, Abudawoud RH, Al-Yami MA, Al-Khattaf SS (2013) *Appl Catal A* 467:224
- Martin C, Malet P, Solana G, Rives V (1998) *J Phys Chem B* 102:2759
- Xin-Li Y, Wei-Lin D, Ruihua G, Kangnian F (2007) *J Catal* 249:278